

Stellar halos and elliptical galaxy formation: Origin of dynamical properties of the planetary nebular systems

Kenji Bekki^{1*} and Eric W. Peng²

¹*School of Physics, University of New South Wales, Sydney 2052, NSW, Australia*

²*Herzberg Institute of Astrophysics, 5071 West Saanich Road, Victoria, BC V8V 2X6, Canada*

Accepted, Received 2005 February 20; in original form

ABSTRACT

Recent spectroscopic observations of planetary nebulae (PNe) in several elliptical galaxies have revealed structural and kinematical properties of the outer stellar halo regions. In order to elucidate the origin of the properties of these planetary nebula systems (PNSs), we consider the merger scenario in which an elliptical galaxy is formed by merging of spiral galaxies. Using numerical simulations, we particularly investigate radial profiles of projected PNe number densities, rotational velocities, and velocity dispersions of PNSs extending to the outer halo regions of elliptical galaxies formed from major and unequal-mass merging. We find that the radial profiles of the project number densities can be fitted to the power-law and the mean number density in the outer halos of the ellipticals can be more than an order of magnitude higher than that of the original spiral's halo. The PNSs are found to show a significant amount of rotation ($V/\sigma > 0.5$) in the outer halo regions ($R > 5R_e$) of the ellipticals. Two-dimensional velocity fields of PNSs are derived from the simulations and their dependences on model parameters of galaxy merging are discussed in detail. We compare the simulated kinematics of PNSs with that of the PNS observed in NGC 5128 and thereby discuss advantages and disadvantages of the merger model in explaining the observed kinematics of the PNS. We also find that the kinematics of PNSs in elliptical galaxies are quite diverse depending on the orbital configurations of galaxy merging, the mass ratio of merger progenitor spirals, and the viewing angle of the galaxies. This variation translates directly into possible biases by a factor of two in observational mass estimation. However, the biases in the total mass estimates can be even larger. The best case systems viewed edge-on can appear to have masses lower than their true mass by a factor of 5, which suggests that current observational studies on PNe kinematics of elliptical galaxies can significantly underestimate their real masses.

Key words: galaxies:halos — galaxies:elliptical and lenticular, cD — galaxies:individual (NGC 5128) — galaxies:kinematics and dynamics — galaxies:stellar content

1 INTRODUCTION

Structural, kinematical, and chemical properties of stars in the outer regions of galaxies, their halos, provide vital clues to their global formation and evolutionary histories. Although the physical properties of stellar halos have been extensively investigated mostly for spiral (e.g., the Galaxy and the M31) and dwarf galaxies in the Local Group (e.g., Eggen, Lynden-Bell, & Sandage 1962; Mould & Kristian 1986; Norris 1986; Freeman 1987; Durrell, Harris, &

Pritchett 1994, 2001; Pritchett & van den Bergh 1998; Reitzel, Guhathakurta, & Gould 1998; Grillmair et al. 1996; Chiba & Yoshii 1998; Davidge 2002), recent observations have started to reveal physical properties of stellar halos in giant elliptical galaxies, all of which are beyond the Local Group (e.g., Soria et al. 1996; Harris, Harris, & Poole 1999 hereafter referred to as HHP; Harris & Harris 2000, HH00; Harris & Harris 2002, HH02; Marleau et al. 2000; Rejkuba et al. 2002; Gregg et al. 2004). These data prompt us to investigate how the properties of stellar halos can be used to understand the formation of giant elliptical galaxies.

* E-mail: bekki@bat.phys.unsw.edu.au

Beyond projected radii of $\sim 2R_e$, it becomes very diffi-

cult to study the integrated properties of stars in ellipticals because of the low stellar surface brightness. Hence, studies of stellar halos tend to rely on resolving individual stars or star clusters. While there are significant observational difficulties in revealing the three dimensional structure and kinematics of halo red giants and AGB stars, it has been possible to use color-magnitude diagrams to derive their metallicity distribution function (hereafter MDF) and constrain the past star formation and chemical evolution histories of their host elliptical galaxies (e.g., HHP; HH00, HH02). Kinematic properties of these stars, however, which can contain vital clues to both structure and formation of ellipticals, are still extremely difficult to obtain. Furthermore, these previous observations have difficulties in deriving *global* stellar halo distributions, which are also considered to have valuable information on the past merging histories of galaxies (e.g., fossil tidal streams), mainly because the halo fields investigated cover only a minor portion of the entire halo.

Planetary nebulae (PNe) are a valuable complement to integrated light and red giant studies. They are powerful tools for studying the dynamical states of elliptical galaxies, because we can more readily identify PNe through their bright [O III] emissions lines and typically measure their radial velocities to an accuracy of $\sim 15 \text{ km s}^{-1}$ (e.g., Peng et al. 2004a, PFF04a). Spectroscopic observations of the radial velocities of PNe in several nearby elliptical galaxies therefore have succeeded in deriving global mass distributions and velocity fields of these galaxies (Ciardullo et al. 1993; Hui et al. 1995; Arnaboldi et al. 1998; Mendez et al. 2001; Romanowsky et al. 2003; Napolitano et al. 2004; PFF04a). For example, kinematic information of PNe in the stellar halo of NGC 5128 at radii up to $\sim 80 \text{ kpc}$ allows the authors to derive the zero velocity curve (ZVC) in the two-dimensional velocity field of the PNS and thereby to discuss the triaxial shape of the mass distribution of this galaxy (PFF04a). This observed diversity in kinematics of PNSs is providing fresh clues to the origin of early-type galaxies. (Romanowsky et al. 2003; PFF04a).

In spite of this importance of PNe studies in elliptical galaxies, only a few theoretical and numerical attempts have been made to discuss dynamical properties of PNSs in elliptical galaxies. For example, using kinematical data up to $\sim 6R_e$ for an heterogeneous sample of elliptical galaxies, Napolitano et al. (2004) derived the dependences of the radial gradients of the mass-to-light-ratios on the B -band magnitude of the galaxies and thereby discussed whether the derived dependences can be consistent with elliptical galaxy formation models based on a Λ CDM model. However, PNSs provide a very rich data set from which to study ellipticals. In particular, we are interested in exploring *the 2D distributions of structural and kinematical properties of PNSs*, which can provide some vital clues both to the triaxial shapes of the global mass distributions of galaxies and to their formation processes. The origin of 2D structural and kinematical properties of PNSs extending to the outer halo regions of elliptical galaxies remains unclear. Furthermore providing theoretical predictions on dynamical properties of PNSs will help to interpret the properties of PNSs that will be obtained in future systematic observations for elliptical galaxies.

The purpose of this paper is thus to investigate structural and kinematical properties of PNSs of elliptical galax-

ies based on numerical simulations. In order to elucidate the origin of the observed properties of the PNSs, we adopt the merger scenario (Toomre 1977) in which elliptical galaxies are proposed to be formed by major merging of two spiral galaxies. The present numerical investigation is two-fold as follows. We first describes radial profiles of structural and kinematical properties of PNSs and two-dimensional (2D) velocity fields of PNSs in elliptical galaxies and their dependences on model parameters. We then compare the simulated kinematics of the PNSs with the corresponding observations for NGC 5128 and thereby try to provide the best model for the PNS in NGC 5128 and discuss advantages and disadvantages of the model in explaining the kinematics of the PNS self-consistently. The essential reason for our choice of the NGC 5128 PNS is that PFF04a have recently investigated radial velocities of the NGC 5128's 780 PNe (among 1141 PNe), which represents the largest kinematical study of an elliptical galaxy to date and thus can be compared with our simulations in the most self-consistent manner. Furthermore, the present study is complimentary to those by Bekki et al. (2003, BHH03) and Beasley et al. (2003) which numerically and semi-analytically investigated the MDF of the stellar halo of NGC 5128 but did not investigate the dynamical properties.

In the present paper, we mainly investigate structural and kinematic properties of PNSs for a large radial extent in elliptical galaxies ($0 \leq R \leq 10R_e$), which include the outer faint stellar halos and the main bodies of the galaxies. Although previous numerical simulations investigated spatial distributions and the line-of-sight velocity distributions of stars in elliptical and S0 galaxies formed from merging for $R < 2.5R_e$ (e.g., Bendo & Barnes 2000; Cretten et al. 2001; Naab & Trujillo 2005), they did not investigate the dynamical properties for the outer halo regions of elliptical galaxies. Therefore, the present numerical results on the dynamical properties of the outer stellar halos including PNe ($5R_e \leq R \leq 10R_e$) may provide new clues to elliptical galaxy formation. Physical properties of these halo stars may well have fossil information on angular momentum redistribution of stars (or conversion from galactic orbital angular momentum into intrinsic angular momentum) which is an essential physical process of galaxy merging. We therefore can expect that dynamical properties of stellar halos, which can be provided by studies of PNSs, may depend strongly on physics of galaxy merging. Through the course of this paper, we thus interpret our simulations in the context of the capabilities of present-day PN surveys in order to facilitate the comparison between theory and observations.

The plan of the paper is as follows: In the next section, we describe our numerical models for the formation of PNSs extending to the outer halo regions in galaxy mergers. In §3, we present the numerical results mainly on the final 2D distributions of structural and kinematical properties in merger remnants (i.e., elliptical galaxies) for variously different merger models. In §4, we compare the simulated results of PNSs with observations of the PNS in NGC 5128 (Cen A). In §5, we discuss whether physical properties of stellar halos can give any constraints on galaxy formation, based on the present numerical results. In this section, we also discuss possible different properties of PNSs in galaxies with different Hubble types. We summarize our conclusions in §6.

Table 1. Model parameters

Model no.	Orbital type	m_2	Comments
M1	–	–	isolated disk
M2	HI	1.0	fiducial model
M3	PP	1.0	
M4	RR	1.0	
M5	LA	1.0	
M6	BO	1.0	
M7	HI	0.1	
M8	HI	0.3	
M9	PO	0.5	NGC 5128 model
M10	–	1.0	Multiple merger

2 MODEL

2.1 Merger models

We investigate the dynamical evolution of fully self-gravitating galaxies composed of stars and dark matter via collisionless numerical simulations carried out on a GRAPE board (Sugimoto et al. 1990). Since our numerical methods for modeling dynamical evolution of galaxy mergers have already been described by Bekki & Shioya (1998) and by BHH03, we give only a brief review here. The total mass and the size of a disk of the merger progenitor spiral are M_d and R_d , respectively. Henceforth, all masses and lengths are measured in units of M_d and R_d , respectively, unless specified. Velocity and time are measured in units of $v = (GM_d/R_d)^{1/2}$ and $t_{\text{dyn}} = (R_d^3/GM_d)^{1/2}$, respectively, where G is the gravitational constant and assumed to be 1.0 in the present study. If we adopt $M_d = 6.0 \times 10^{10} M_\odot$ and $R_d = 17.5$ kpc as a fiducial value, then $v = 1.21 \times 10^2$ km/s and $t_{\text{dyn}} = 1.41 \times 10^8$ yr, respectively. The merger progenitor spiral is composed of a dark matter halo, a stellar disk, a stellar bulge, and a stellar halo.

The mass ratio of the dark matter halo to the stellar disk in a disk model is fixed at 10 for all models. We adopt the density distribution of the NFW halo (Navarro, Frenk & White 1996) suggested from CDM simulations:

$$\rho(r) = \frac{\rho_0}{(r/r_s)(1+r/r_s)^2}, \quad (1)$$

where r , ρ_0 , and r_s are the spherical radius, the central density of a dark halo, and the scale length of the halo, respectively. The value of r_s (0.6 in our units for $c = 10$) is chosen such that the rotation curve of a disk is reasonably consistent with observations. The mass fraction and the scale length of the stellar bulge are fixed at 0.17 (i.e., 17 % of the stellar disk) and 0.04 (i.e., 20 %) of the scale length of the stellar disk, respectively, which are consistent with those of the bulge model of the Galaxy. The initial total mass of the stellar halo is 0.01 in our units for all models and has a number density distribution ($\rho(r) \sim r^{-3.5}$) like that of the stellar halo of the Milky Way (e.g., Chiba & Beers 2000).

The total number of collisionless particles in each simulation is 112680 for pair mergers and 281700 for multiple merger (described later). The total particle number for dark matter halo, stellar disk, bulge, stellar halo, and old halo GCs are 30000, 20000, 3340, 2000, and 1000, respectively, for a disk. Gravitational softening lengths in the GRAPE simulations are set to be fixed at 0.15 (in our units) for the dark matter, 0.02 for the stellar disk and bulge, 0.09 for the stellar halo for each simulation. Since we mainly analyze

structural and kinematical properties of PNSs for the scale of 1 – 100kpc in galaxies, the resolution of the simulations (~ 350 pc) is quite reasonable.

We investigate both pair mergers with the number of the progenitor spirals (N_g) equal to 2 and multiple ones with $N_g = 5$. Since our main interest here is the formation of elliptical galaxies by pair mergers, the details of the models and the results for the multiple mergers are given in the Appendix B. In the simulation of a pair merger model, the orbit of the two spirals is set to be initially in the x - y plane and the distance between the center of mass of the two spirals (r_{in}) is $6R_d$ (105 kpc). The pericentre distance (r_p) and the orbital eccentricity (e_p) are assumed to be free parameters which control orbital angular momentum and energy of the merging galaxies. For most merger models, r_p and e_p are set to be 1.0 (in our units) and 1.0, respectively. The spin of each galaxy in a merging and galaxy is specified by two angles θ_i and ϕ_i (in units of degrees), where the suffix i is used to identify each galaxy. Here, θ_i is the angle between the z -axis and the vector of the angular momentum of the disk, and ϕ_i is the azimuthal angle measured from x axis to the projection of the angular momentum vector of the disk onto the x - y plane.

We specifically show the following five different and representative models with different disk inclinations with respect to the orbital plane: A prograde-prograde model represented by “PP” with $\theta_1 = 0$, $\theta_2 = 30$, $\phi_1 = 0$, and $\phi_2 = 0$, a retrograde-retrograde (“RR”) with $\theta_1 = 180$, $\theta_2 = 150$, $\phi_1 = 0$, and $\phi_2 = 0$, and a highly inclined model (“HI”) with $\theta_1 = 30$, $\theta_2 = 120$, $\phi_1 = 90$, and $\phi_2 = 180$. The model with lower orbital angular momentum ($r_p = 0.2$) and a HI orbital configuration is labeled as “LA” whereas the model with bound orbit with e_p of 0.7 and a HI orbital configuration is labeled as “BO”.

The total masses of elliptical galaxies can be underestimated, if kinematical properties of PNSs are used for the mass estimation (e.g., Dekel et al. 2005). We also find that the masses of ellipticals can be significantly underestimated if radial velocity profiles of PNSs are used under the assumption of the virial theorem. We just briefly discuss this point in the discussion section §5.3, because our main focus is on 2D density and velocity fields of PNSs in elliptical galaxies.

2.2 Main points of analysis

We mainly investigate 2D density and velocity fields of PNSs and compare the results with the corresponding observations in a fully self-consistent manner. We accordingly use Gaus-

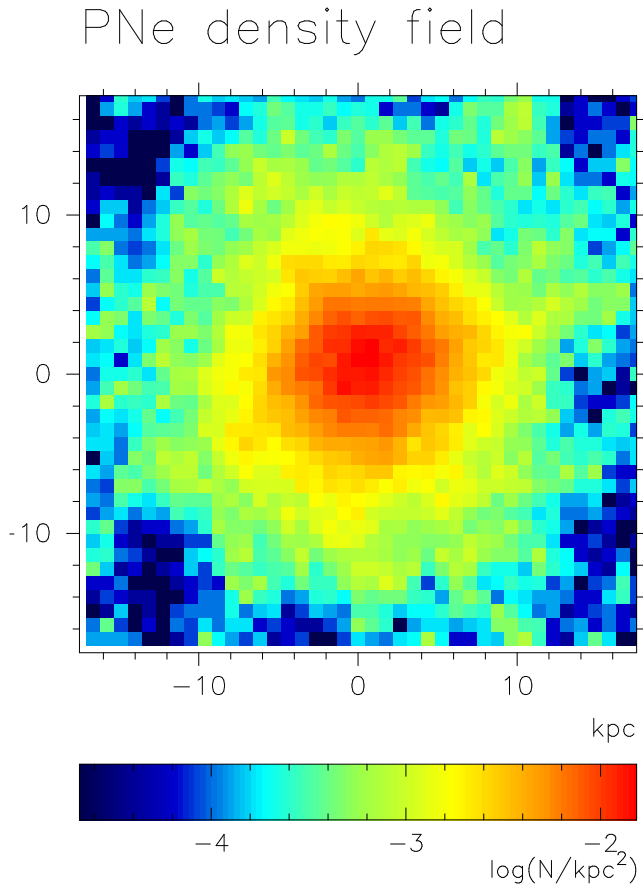


Figure 1. The two-dimensional (2D) PNe density field of the stellar halo in the isolated disk model M1 projected onto the X - Y plane. The stellar halo region with the size of 17.5 kpc is divided into 40×40 cells and the projected PNe density at each cell is estimated by assuming α_{PNe} of 9.4×10^{-9} PNe per L_{\odot} in B -band (Ciardullo et al. 1989). The original spherical distribution of the PNS is clearly seen in this smoothed 2D density field.

sian smoothing similar to that adopted in observations (e.g., PFF04a) in order to derive smoothed density and velocity fields of the simulated PNSs. The details of the methods to derive the smoothed fields are given in the Appendix A. Figure 1 shows how the smoothed PNe density field looks like for the stellar halo consisting only of 1000 discrete stars in an isolated disk model M1 (viewed from face-on).

Although the MDFs of stellar halos (thus PNe) can give some constraints on any theory of elliptical galaxies formation (e.g., HH00; HH02; BHH03), we do not intend to discuss them in this paper. This is firstly because (1) the importance of the MDFs have been already discussed in previous papers (e.g., BHH03) and secondly because there is no currently available data set of the MDFs of PNe for nearby giant elliptical galaxies. Instead, we mainly investigate (1) radial profiles of projected PNe number densities, (2) 2D fields of line-of-sight velocity (V_{los}) and velocity dispersion (σ), (3) rotation curve profiles (V_{rot}), and (4) radial profiles of σ and V_{rot}/σ , for the PNSs of merger remnants. Although we investigated the above four points for 32 merger models with different m_2 and orbital configurations, we show the results of 9 representative models among them. Table 2 summarizes the model parameters used for these 9 models. We show the

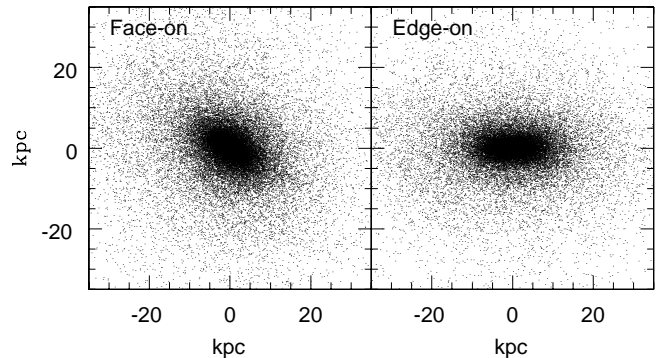


Figure 2. The mass distributions of stars projected onto the X - Y plane (face-on view, left) and the X - Z one (edge-on view, right) for the fiducial model M2 at $T = 4.5$ Gyr.

results of the models at $T = 4.5$ Gyr (at final time step), where the time T represents time that has elapsed since the merger progenitor disks begin to merge.

We firstly show the results of the “fiducial model”, model M2, which show typical behaviors of stellar halo (thus PNS) formation in major galaxy merging (§3.1). The results of this model can be regarded as generic ones for elliptical galaxies formed from major merging. Secondly we show the parameter dependences of the results in §3.2 with special emphasis on the dependence of projected PNe number densities and the 2D velocity fields on orbital configuration and m_2 . Thirdly, we present the best model which can reproduce the most reasonably well a number of dynamical properties of the PNS observed in NGC 5128 (§4.1). It should be stressed here that the best model is the best model *among the present 32 models*, thus is not the one which reproduce all of the observed properties of the PNS fully self-consistently. We try to understand advantages and disadvantages of the present best model by comparing it with observations, and discuss whether (and how) physical effects that are not included in the present models (e.g., star formation) can be important for more successful reproduction of the observations. The best model is model M9 with $e_p = 1.0$, $r_p = 0.05$ in our units, $\theta_1 = 0$, $\theta_2 = 80$, $\phi_1 = 0$, and $\phi_2 = 0$, and $m_2 = 0.5$ (The orbital configuration is hereafter referred to as “PO”).

3 RESULTS

3.1 The fiducial model

3.1.1 Density fields

Figure 2 shows the projected stellar mass distributions of the fiducial model M2 at $T = 4.5$ Gyr in which the final merger remnant shows R_e of 5.2 kpc, $L_B = 3.7 \times 10^{10} L_{\odot}$, and $N_{\text{PNe}} = 350$ within $\sim 5R_e$. The merger remnant does not show any clear signs of stellar substructures (i.e.tidal tails and plums) in its halo region for the two projections owing to the apparently completed dynamical relaxation by this time ($T = 4.5$ Gyr). It is also possible that the much less remarkable substructures are due to the adopted smaller particle number (an order of $\sim 10^5$). The outer stellar halo ($R > 5R_e$) in the edge-on view is more spherical ($\epsilon \sim 0.3$) than the main body of the elliptical ($\epsilon \sim 0.2$ at $R \sim 2R_e$).

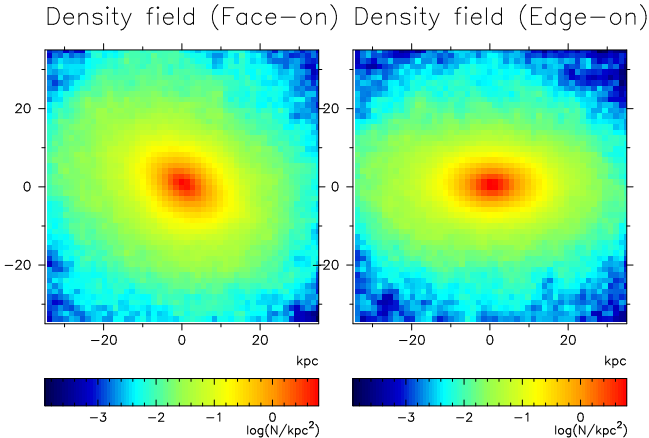


Figure 3. The 2D PNe density field for the face-on view (left) and the edge-on view (right) in the fiducial model at $T = 4.5$ Gyr. The 2D fields are produced based on the stellar mass distributions shown in Figure 2.

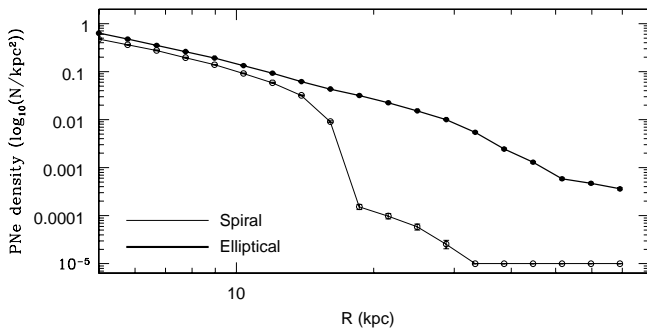


Figure 4. Radial profiles of the projected PNe number densities (ρ_{PNe}) for the fiducial merger model M2 (thick) and the isolated disk model M1 (thin). Note that the elliptical galaxy formed in M2 shows significantly higher ρ_{PNe} in its outer region ($R > 20$ kpc) compared with the spiral in M1.

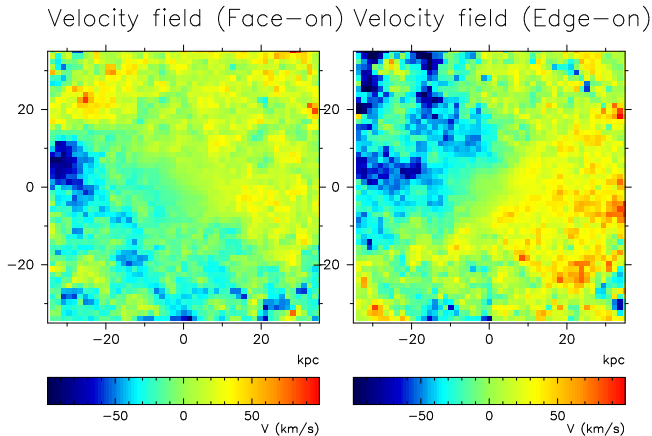


Figure 5. The 2D velocity fields for the face-on view (left) and for the edge-on view (right) for the fiducial model M2 at $T = 4.5$ Gyr.

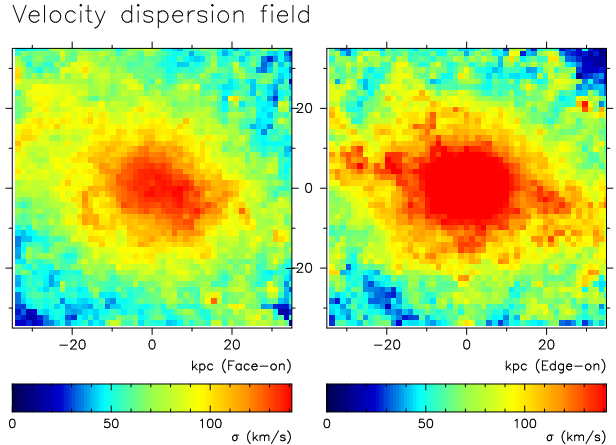


Figure 6. The same as Figure 5 but for the 2D velocity dispersion fields.

The outer stellar halo is slightly more flattened than the dark matter halo with $\epsilon = 0.15$ at $R = 5R_e$ in the edge-on view and the major-axis of the stellar halo nearly coincides with that of the dark matter halo. The isophotal shape of this remnant formed from purely collisionless major galaxy merging can show the negative sign of the a_4 parameter (e.g., Bekki & Shioya 1997), and thus this remnant can be morphologically identified as a boxy elliptical galaxy.

Figures 3 and 4 describe the 2D density fields of the PNS in the elliptical and the radial profile of the PNe distribution, respectively. Owing to the adopted assumption of constant α_{PNe} (i.e., constant luminosity-specific number densities of PNe), the 2D density fields of the PNS follows the stellar density ones of the elliptical and therefore shows a more flattened shape in the edge-on view. The radial density profile is best fitted to the power-law with the exponent of -2.7 for $0 \leq R \leq 40$ kpc ($\sim 8R_e$), which is slightly steeper than the observed slope of -2.5 for the PNS of NGC 5128 (PFF04a). The projected PNe density of the elliptical in its outer stellar halo ($R > 5R_e$) is more than two orders magnitudes higher than those of the merger progenitor spirals, though the PNe densities in the central regions of galaxies are not so different between the elliptical and the spirals. The formation of such a high density stellar halo is demonstrated to be closely associated with redistribution of disk stars through tidal stripping of the stars during major galaxy merging (BHH).

Figure 5 shows the 2D fields of V_{los} (i.e., line-of-sight-velocity) of the merger remnant for $0 \leq R \leq 35$ kpc ($\sim 7R_e$) in the face-on and edge-on views. Clearly, the PNS shows a significant amount of rotation (~ 100 km s $^{-1}$) along its major axis (i.e., the X -axis) for the edge-on view. Given the fact that the stellar halos of the merger progenitor spirals are assumed to have no net rotation, the rotation in the outer halo of the elliptical can be considered to be obtained during angular momentum redistribution of major galaxy merging. This angular momentum transfer processes have been already well discussed in previous papers (e.g., Barnes 1998 for a review).

The axis of rotation in the edge-on view however does not coincide with the minor axis of the PNe density field shown in Figure 3: Radial velocity gradient can become maximum if we measure it along a line connecting two points (X ,

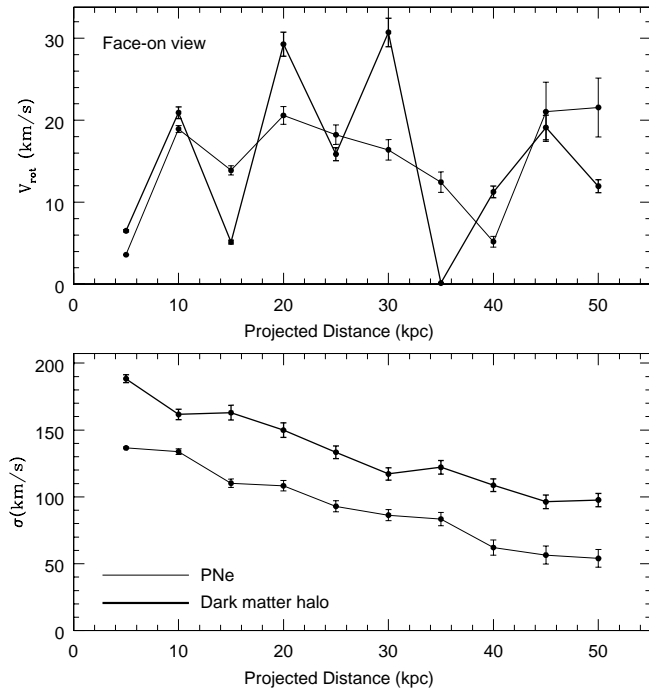


Figure 7. The radial profile of the rotation curve V_{rot} (upper) and the velocity dispersion σ (lower) for the dark matter halo (thick) and for stars (thin) in the fiducial model M2 at $T = 4.5$ Gyr. V_{rot} and σ are estimated for the model projected onto the X - Y plane (i.e., the face-on view). The methods to derive V_{rot} and σ and their error bars are described in detail in the Appendix A.

Z) = $(-35, 35)$ and $(35, -35)$ kpc for the edge-on 2D velocity field. Minor axis rotation can be clearly seen in the outer halo region of the elliptical for the edge-on 2D velocity field and the velocity variation along the minor axis (i.e., the Z -axis) is complicated. Also it should be stressed that the edge-on 2D field has several regions with large absolute magnitudes of V_{los} (e.g., $(X, Z) = (35, -8)$ and $(-20, 3)$ kpc). Such inhomogeneity in the velocity space may indicate that dynamical relaxation is not completely ended in a real term even a few Gyr after the coalescence of two spirals in the fiducial model: Fossil evidences of past violent relaxation can be proved in velocity structures of outer stellar halos in elliptical galaxies.

The face-on 2D velocity field also shows rotation along the major and the minor axes of the projected density distribution of the PNS, though the rotation in the outer stellar halo for the face-on 2D field is less remarkable compared with the edge-on one. The global appearance of the face-on 2D velocity field is smoother than that of the edge-on one and complicated velocity variation along the minor axis of the PNS can not be clearly seen. Thus these results imply that (1) PNSs in elliptical galaxies can show a significant amount of rotation in their outer halo regions, (2) minor-axis rotation of PNSs is one of important characteristics of elliptical galaxies, and (3) the 2D velocity fields can be different for different viewing angles.

As shown in Figure 6, both the face-on and the edge-on 2D velocity dispersion (σ) fields show (1) higher velocity dispersion in the inner regions of the elliptical, (2) a shallower gradient of velocity dispersion along the major axis

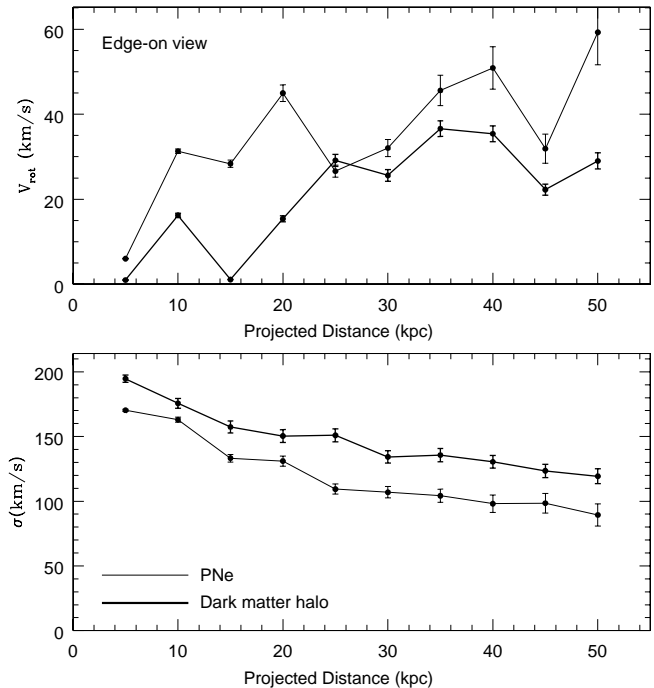


Figure 8. The same as Figure 7 but for the edge-on view (i.e., the X - Z plane).

(i.e., the X -axis) compared with that along the minor one, and (3) globally flattened shapes, in particular, in outer stellar halo regions. These three can be regarded as important kinematical characteristics of stellar halos (PNSs) in elliptical galaxies formed by major merging. The flattened velocity dispersion fields are due to anisotropic velocity dispersion in the triaxial mass distribution of the elliptical galaxy in this fiducial model. The dispersion field appears to be more homogeneous in the face-on view than in the edge-on one, though some remarkable substructures that can result from yet incomplete dynamical relaxation of this system can be seen in both projections. The results shown in Figures 4, 5, and 6 clearly suggest that even if the 2D density fields of PNSs appear to be quite regular and axisymmetric, their 2D velocity and velocity dispersion fields can be more inhomogeneous and less axisymmetric: The kinematical properties of a stellar halo in an elliptical galaxy can provide some evidences of the past dynamical processes of its formation, if penetrative analysis of such “fossil record” properties can be done.

Figures 7 and 8 show the radial profiles of rotational velocities (V_{rot}) and velocity dispersions (σ) for the dark matter halo and the stellar components (i.e., PNe) in the elliptical of the fiducial model. It is clear from these figures that (1) the dark matter halo shows a larger velocity dispersion (by a factor of 1.1 – 2.0, depending on radius) than the PNe, (2) the PNe shows a significant amount of rotation 40 – 60 km s^{-1} in the entire halo region ($R > 5R_e$) of the elliptical for the edge-on view, (3) the maximum V_{rot} in the halo region is higher in the edge-on view than in the face-on one, (4) the radial gradient of V_{rot} is quite different between different projections, and (5) the radial velocity dispersion profiles (e.g., the central σ and the gradient) do not differ significantly with each other. The above result (1) strongly

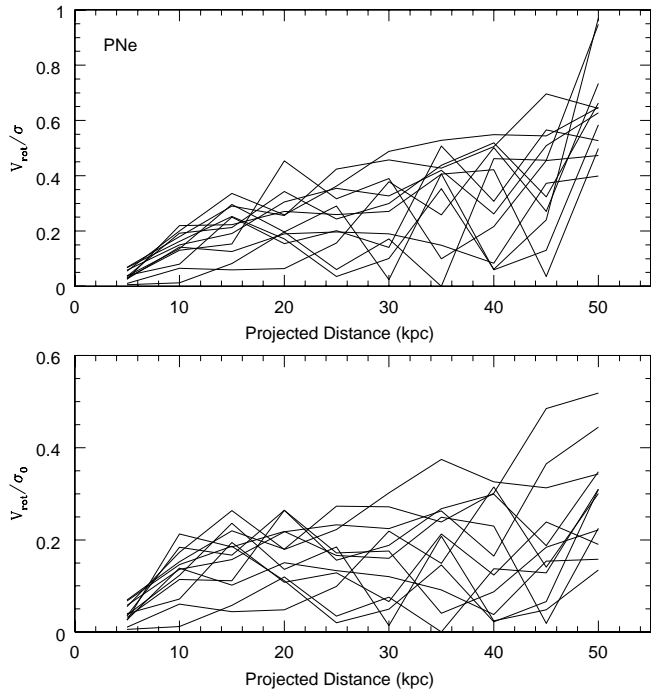


Figure 9. The radial profiles of V_{rot}/σ (upper) and the normalized rotation curve V_{rot}/σ_0 (lower) for the fiducial model viewed from 12 representative, and different viewing angles. Note that there is a trend of increasing V_{rot}/σ and V_{rot}/σ_0 with radius.

suggests that we can significantly underestimate the total mass of an elliptical galaxy, if we use only the velocity dispersion data of the PNS and thereby derive the total mass based on the scalar virial theorem in which the mass is linearly proportional to the product of R_e and σ : We need to derive the total mass of an elliptical by using both dispersion and rotation data of the PNS. The result (2) is consistent with previous numerical simulations (e.g., Heyl et al. 1996).

Given the fact that the radial dispersion profile of the PNS decreases with radius in the fiducial model, the above result (2) means that the PNS shows a higher value of V_{rot}/σ in the outer halo of the elliptical. (e.g., V_{rot}/σ of ~ 0.7 at $R \simeq 5R_e$). This larger V_{rot}/σ also results from the redistribution of angular momentum of disks stars during major merging (i.e., conversion of initial orbital angular momentum of merger progenitor disks into final intrinsic one of the merger remnant), as explained for Figure 5. This result suggests that larger V_{rot}/σ in the outer stellar halo of an elliptical galaxy can be a fossil evidence that the elliptical was formed from major galaxy merging. The derived PNS with larger V_{rot}/σ in the outer halo region is in a striking contrast to the Galactic stellar halo with little rotation (e.g., Freeman 1987), which implies that stellar halo kinematics can be significantly different between spirals and ellipticals. Recent numerical simulations based on the currently favored cold dark matter (CDM) theory of galaxy formation have shown that the Galactic stellar halo with little rotation is formed at high redshift ($z > 1$) by dissipative and dissipationless merging of smaller subgalactic clumps and their resultant tidal disruption in the course of gravitational contraction of the Galaxy (Bekki & Chiba 2000, 2001). Thus the above result (2) implies that differences in formation processes of

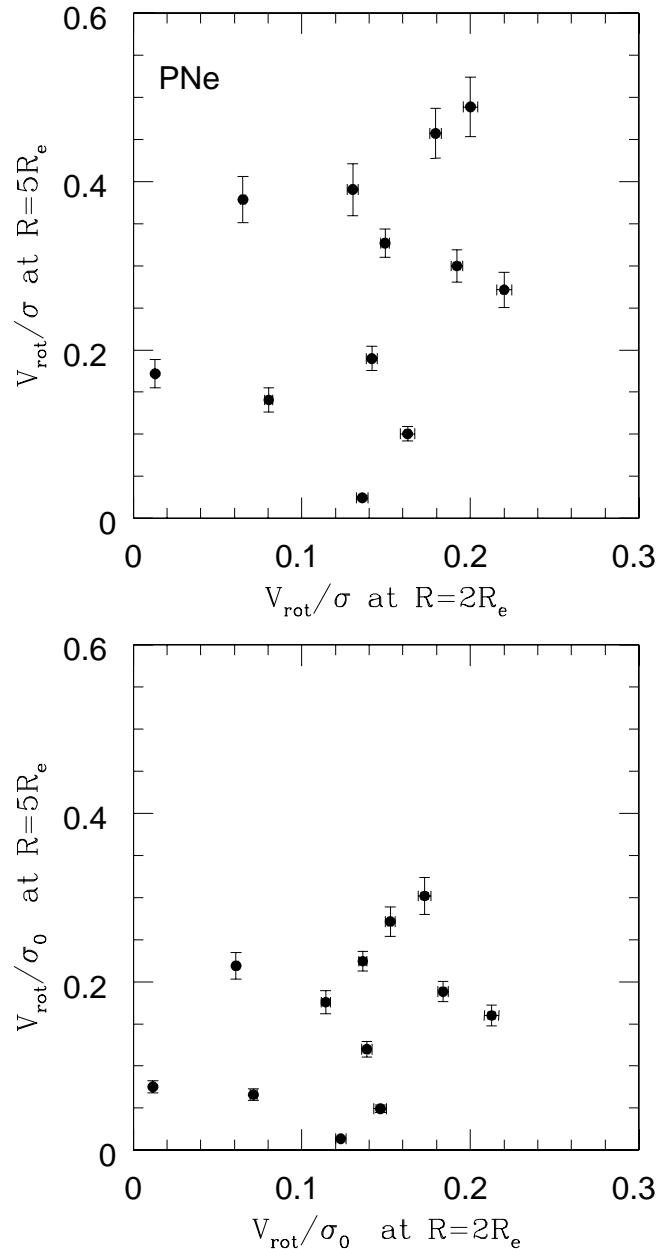


Figure 10. V_{rot}/σ at $R = 5R_e$ as a function of V_{rot}/σ at $R = 2R_e$ (upper) and V_{rot}/σ_0 at $R = 5R_e$ as a function of V_{rot}/σ_0 at $R = 2R_e$ (lower) for the fiducial model viewed from 12 representative, and different directions.

stellar halos between different types of galaxies (e.g., spirals vs ellipticals) can be reflected on the stellar halo kinematics. The above results (3) - (5) imply that radial profiles of rotational velocities of PNSs in elliptical galaxies depend more strongly on viewing angles than those of velocity dispersion.

Figure 9 describes how V_{rot}/σ and V_{rot}/σ_0 depend on radius in the PNS of the fiducial model for 12 representative projections. There can be seen a trend of increasing V_{rot}/σ and V_{rot}/σ_0 with increasing radius, though the radial profiles rise and fall with radius significantly. The higher V_{rot}/σ and V_{rot}/σ_0 of the PNS in the outer halo region of the elliptical for most of the projections (viewing angles) means that the PNS in the outer halo region is the most likely to

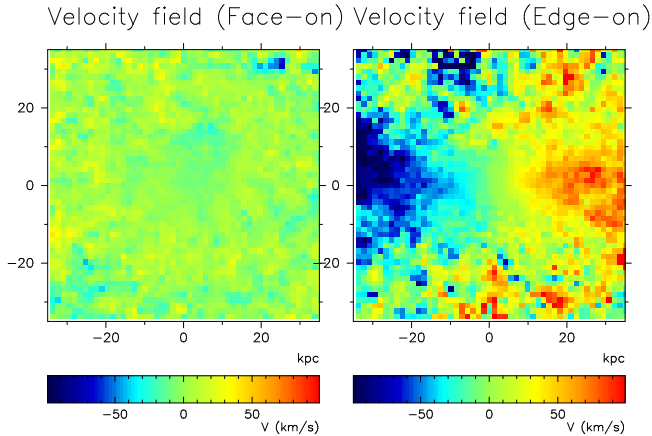


Figure 11. The 2D velocity fields for the face-on view (left) and for the edge-on view (right) for the model M3 at $T = 4.5$ Gyr.

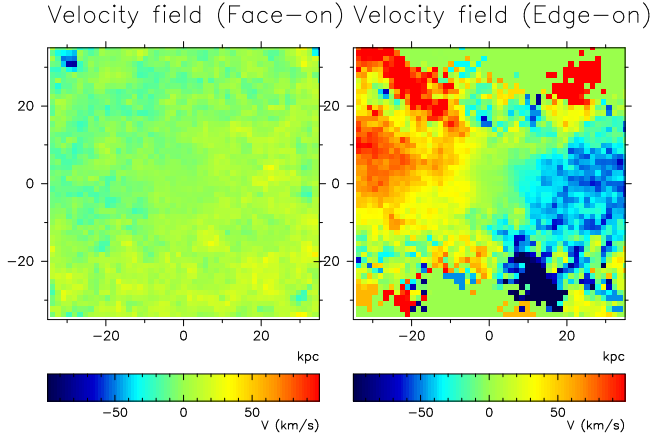


Figure 12. The same as Figure 11 but for the model M4.

be observed as being strongly supported by rotation. Figure 10 shows that a PNS with higher V_{rot}/σ at $R = 2R_e$ is more likely to have higher V_{rot}/σ at $R = 5R_e$: There is a correlation in stellar kinematics between the main body and the stellar halo of the elliptical, though the correlation is weak. Figure 10 also shows a stronger correlation between V_{rot}/σ_0 at $R = 2R_e$ and V_{rot}/σ_0 at $R = 5R_e$. The derived correlations imply that if elliptical galaxies are formed from major galaxy merging, the kinematics of their main bodies derived from integrated absorption spectra (for $R < 2R_e$) can be correlated with that of their outer stellar halos derived from radial velocity fields of PNe (for $R > 5R_e$). The predicted “halo-host kinematic correlation” can be tested by future extensive systematic studies of PNe kinematics for elliptical galaxies with already known kinematics of the main bodies.

3.2 Parameter dependences

3.2.1 Orbital configurations

The dependences of dynamical properties of PNSs in elliptical galaxy formed by major galaxy merging with $m_2 = 1.0$ on orbital configurations of the merging are described as follows.

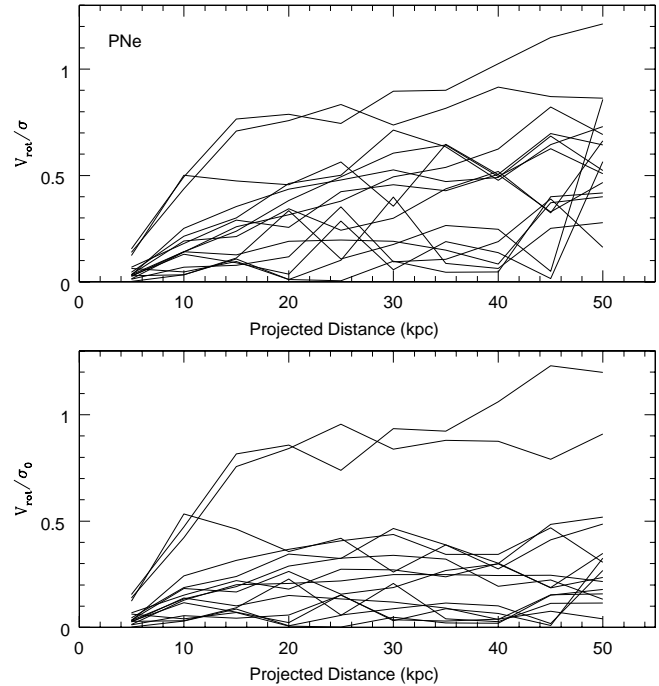


Figure 13. The same as Figure 9 but for the different 5 merger models (M2, M3, M4, M5, and M6) viewed from three different directions (i.e., projected onto the X-Y, X-Z, and Y-Z plane).

(1) Irrespective of orbital configurations, the radial profiles of the projected PNe number densities in PNSs can be fitted to the power-law profile for the entire halo regions of their host elliptical galaxies. The simulated PNSs of ellipticals in all models in the present study have the mean PNe densities more than an order of magnitude higher than those of stellar halos of their merger progenitor spirals. The central values of the projected PNe number densities do not depend on orbital configurations. These results suggest that structural properties of outer PNSs (thus stellar halos) can be significantly different between spirals and ellipticals.

(2) Most of PNSs can show a significant amount of rotation in the outer halo regions ($R > 5R_e$) of their host elliptical galaxies, though the maximum values of the rotational velocities (V_{rot}) depend on the viewing angles of the ellipticals. The 2D velocity fields of most PNSs shows minor-axis rotation in their halo regions, as seen in the main bodies ($R < 2R_e$) of elliptical galaxies (e.g., Bendo & Barnes 2000). The details of the 2D velocity field of PNSs depend strongly on orbital configuration of galaxy merging. For example, the PNS of the elliptical formed from a retrograde-retrograde merging (model M4) shows a more inhomogeneous and more complicated 2D velocity field in its edge-on view than that from a prograde-prograde merging, though there are no significant differences in the 2D fields between the two for the face-on view (See Figures 11 and 12 and compares the two velocity fields with each other). The 2D velocity dispersion fields does not so strongly depend on orbital configurations than the 2D velocity ones.

(3) V_{rot}/σ of PNSs are more likely to be higher in

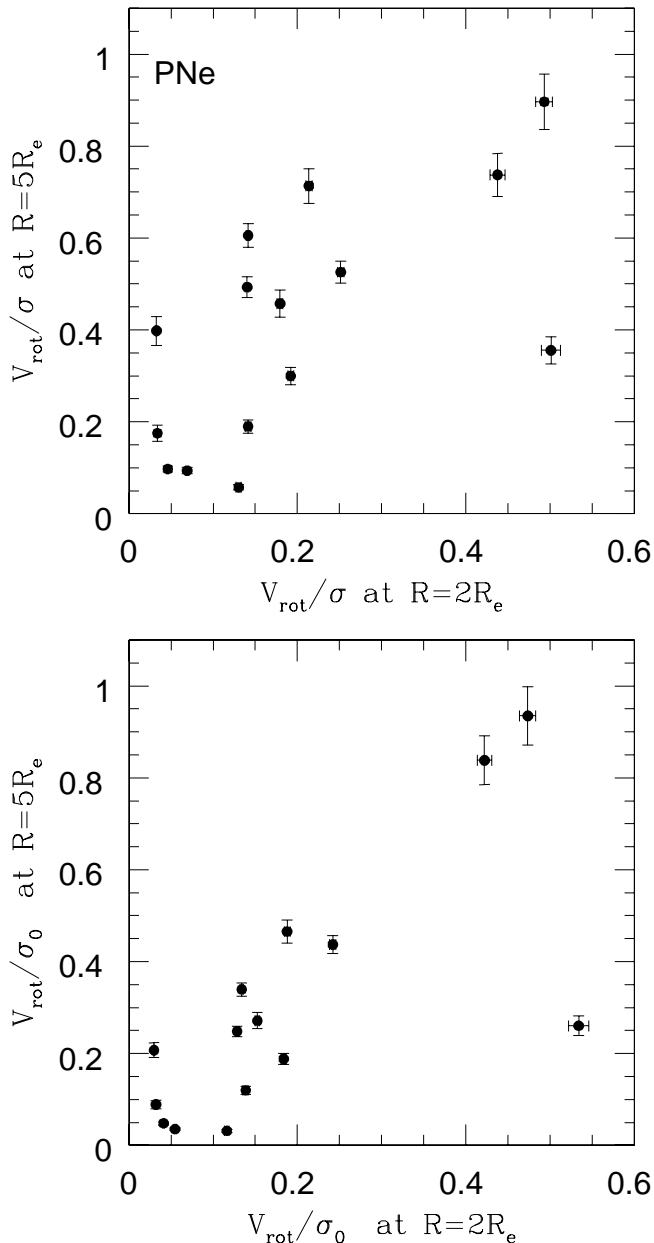


Figure 14. The same as Figure 10 but for the different 5 merger models (M2, M3, M4, M5, and M6) viewed from three different directions (i.e., projected onto the X - Y , X - Z , and Y - Z planes).

the outer halo regions of elliptical galaxies ($R > 25$ kpc corresponding to $\simeq 5R_e$) than in the central regions $R \sim 5$ kpc, as shown in Figure 13. This result suggests that PNSs of elliptical galaxies are likely to show rotational kinematics in their outer halo regions, if they are formed from major galaxy merging. V_{rot}/σ_0 (rotation curve normalized to the central velocity dispersion σ_0) has the radial dependence similar to V_{rot}/σ (Figure 13). The flat rotation curve of V_{rot}/σ_0 seen in most of the models for their outer halo regions ($R > 25$ kpc) suggests that such flattened shapes of V_{rot}/σ_0 is one of generic trends of stellar halos kinematics in elliptical galaxies formed from major merging.

(4) There is a weak correlation between V_{rot}/σ at $R =$

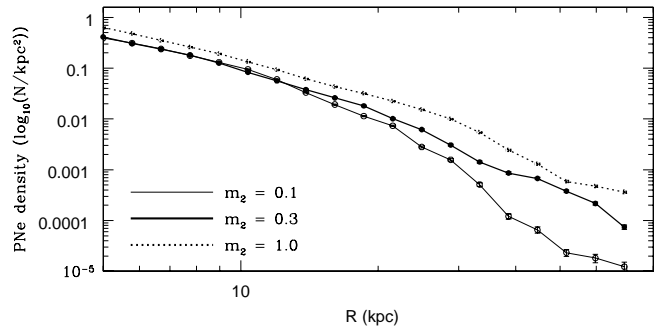


Figure 15. The same as Figure 4 but for the three merger models with different m_2 (M2, M7, and M8).

$2R_e$ and V_{rot}/σ at $R = 5R_e$ in the sense that PNSs with larger V_{rot}/σ at $R = 2R_e$ are more likely to show larger V_{rot}/σ at $R = 5R_e$ (See Figure 14). This result suggests that kinematics of outer stellar halos in elliptical galaxies can correlate with that of their main bodies, if elliptical galaxies are formed from major merging. Similar trend can be seen for V_{rot}/σ_0 , which implies that elliptical galaxies with the main bodies rotating more rapidly are likely to show a larger amount of rotation in their outer halo regions. The derived two correlations, though weak, can be used as theoretical predictions that should be compared with future observations of PNe kinematics in elliptical galaxies.

(5) These radial differences of V_{rot}/σ characteristics of PNSs of elliptical galaxies formed by major merging (See Figures 13 and 14) can be derived *only if we can obtain kinematical data for outer halo components ($R \sim 5R_e$) of elliptical galaxies*. This implies that we need to investigate observationally and theoretically kinematical properties of stellar halos beyond $2R_e$ to give some constraints on elliptical galaxy formation and thus that PNe kinematical studies are ideal for this purpose.

3.2.2 Mass ratios (m_2)

The dependences of dynamical properties of PNSs in merger remnants on m_2 are described as follows.

(1) The projected PNe number densities ρ_{PNe} ($\log_{10}(\text{N}/\text{kpc}^2)$) are globally lower in the remnants with smaller m_2 , in particular, for the outer parts ($R > 5R_e$ corresponding to ~ 25 kpc) of PNSs (See Figure 15). This means that more flattened elliptical galaxies are more likely to show lower ρ_{PNe} , because the morphological properties of the host galaxies formed from these mergers with lower m_2 show more flattened intrinsic shapes. The power-law slope of the density profile ρ_{PNe} ($\log_{10}(\text{N}/\text{kpc}^2)$) does not strongly depend on m_2 for $R \leq 5R_e$, however, there is a clear sign of steeper slope in the model with $m_2 = 0.1$ for $R > 5R_e$ owing to the rather low PNe density there. The result implies that the ρ_{PNe} is steeper in Es formed from major galaxy merging (e.g., $m_2 > 0.3$) than in S0s from unequal-mass/minor galaxy merging with ($0.1 < m_2 < 0.3$).

(2) The kinematics of PNSs in E/S0s formed from galaxy merging with lower m_2 show more rapid rotation, larger maximum values of V_{rot} , and steeper radial gradients of V_{rot} for $R < 2R_e$ (See Figure 16). Given the fact that

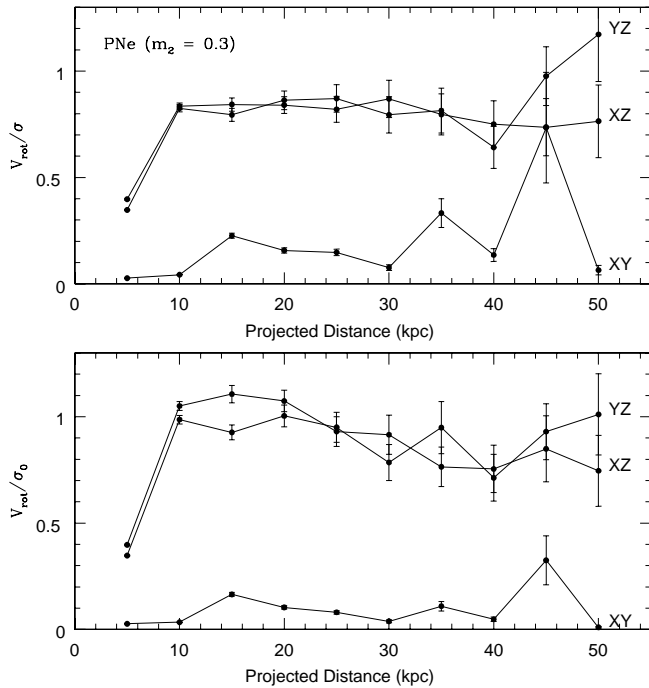


Figure 16. The radial profiles of V_{rot}/σ (upper) and the normalized rotation curve V_{rot}/σ_0 (lower) for the unequal-mass merger model M8 with $m_2 = 0.3$ viewed from three different viewing angles (projected onto the X - Y , X - Z , and Y - Z planes).

remnants of galaxy merging with smaller m_2 show more flattened shapes, this result suggests that more flattened E/S0 have higher V_{rot} and steeper radial V_{rot} gradients. Irrespective of m_2 , the outer regions of PNSs ($R \geq 5R_e$) can show high V_{rot} and thus large V_{rot}/σ , owing to the nearly flat rotation curve and the radially decreasing σ (See Figure 17). This suggests that stellar halos in E/S0s formed by galaxy merging show different kinematics compared with that of the Galaxy with little rotation.

(3) The larger values of V_{rot}/σ in the PNS for edge-on projections (i.e., X - Z and Y - Z) in S0s formed from unequal-mass merging suggests that rotational terms in Jeans equations should be considered when we estimate total masses of S0s using PNe data (See Figure 16). The small values of V_{rot}/σ for the face-on projection (i.e., X - Y) imply that the total mass of an S0 (thus mass-to-light-ratio) can be significantly underestimated if it is viewed from face-on and if the mass is estimated by the Jeans equation with correction terms of rotation (and if the projected central velocity dispersion does not depend on the viewing angle). The observed small M/L in some early-type galaxies (e.g., in NGC 3379) could be due to this viewing angle effect.

4 COMPARISON WITH OBSERVATIONS OF NGC 5128 PNE SYSTEMS

4.1 Selection of the best model

We present the results of one of the best models (model M9) in which the observed structural and kinematical properties of the PNS in NGC 5128 (PFF04a) are the most self-consistently reproduced. We select this best model among

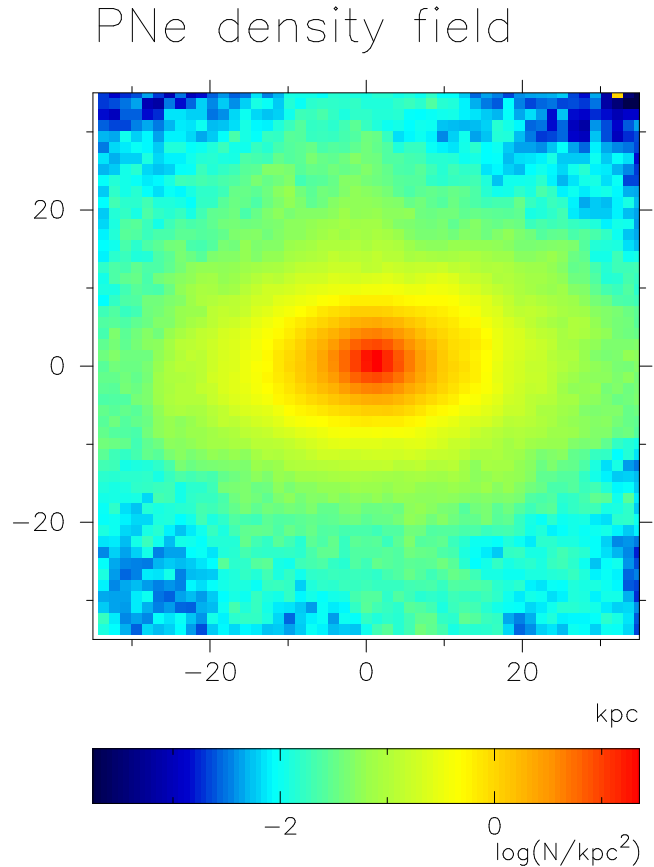


Figure 17. The same as Figure 1 but for the model M9. α_{PNe} of 28.2 PNe per L_\odot in B -band is adopted so that the PNe number density at the effective radius of the merger remnant can be consistent with the observed one for the NGC 5128 PNS.

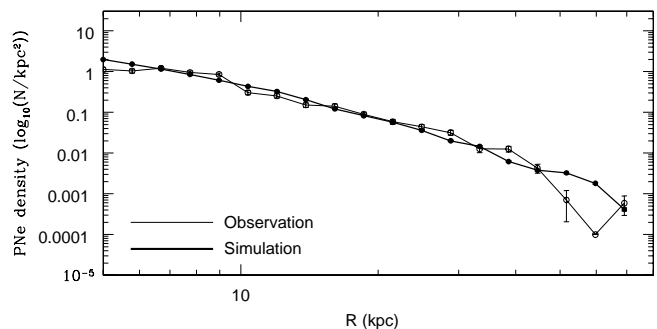


Figure 18. The same as Figure 3 but for and the observational data (thin) by PFF04a and the model M9 (thick).

the 32 models investigated in the present study by checking whether the following five fundamental observational results (e.g., Israel 1998; PFF04a) can be reproduced reasonably well in each model: (1) $R_e = 5.2$ kpc, M_1 (total luminous mass) = $1.4 \times 10^{11} M_\odot$ (for $M_1/L_B = 3.5$), and spherical appearance of the elliptical galaxy, (2) the projected PNe number density ρ_{PNe} ($\log_{10}(\text{N}/\text{kpc}^2) \simeq 1.0$ at $2R_e$ and the slope of the power-law profile similar to -2.5 , (3) the rotation curve that rises till $R \simeq 2R_e$ and becomes flat at $R > 2R_e$ with the maximum V_{rot} of $\simeq 100 \pm 20 \text{ km s}^{-1}$, (4) the central velocity dispersion σ_0 of $\simeq 140 \pm 10 \text{ km s}^{-1}$, and (5)

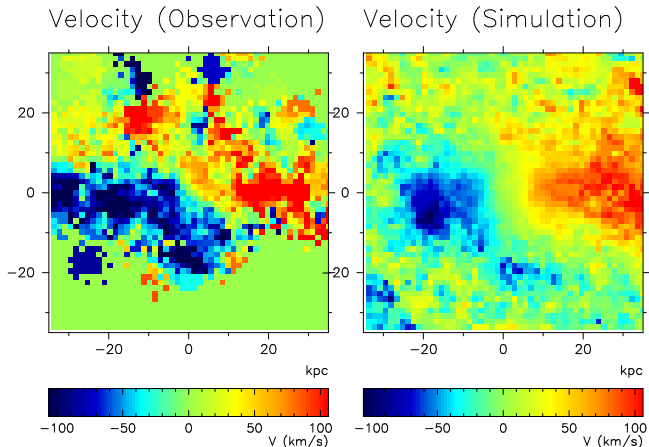


Figure 19. The same as Figure 5 but for the observational data (left) and the model M9 (right).

the 2D velocity field showing both minor and major axes rotation with the zero velocity curve/contour (ZVC) twisting significantly.

Owing to the purely collisionless nature of the present simulations, we can match any model to the above observation (1) by rescaling the size and the mass of the simulation. Therefore, the above (2) - (5) constraints can be used in selecting the best possible model in the present study. Major merger models with $m_2 = 1.0$ can explain the above (2), (4), and (5) reasonable well, however they have difficulties in explaining (3) owing to slowly rising V_{rot} with smaller maximum values of V_{rot} . Unequal-mass merger models with $m_2 = 0.1 - 0.3$ can become early-type E/SOs, however, they are very flattened in shapes, strongly supported by rotation, and have 2D velocity fields that are not similar to the observed ones. These models accordingly can not explain the above (1), (4), and (5) in a *fully self-consistent manner* and thus can not be regarded as the best model. Thus one of the best models can be unequal-mass mergers with m_2 of somewhere between 0.3 and 1.0 (viewed from a certain direction): However, it should be stressed here that we possibly could miss out the major merger model with $m_2 = 1.0$ that can explain the above five points self-consistently, owing to the limited number of the simulated models.

The best model for which we show the results below is the model 9 with $m_2 = 0.5$ in which a highly inclined orbital configuration and a smaller pericentre distance are assumed. We investigate dynamical properties of the PNS in this model at $T = 4.5$ Gyr when the remnant is dynamically well relaxed to show regular distributions of PNe both in the 2D distribution of the projected number density and in the radial one (See Figures 17 and 18). This model with smaller pericenter distance and a highly inclined disk with respect to the orbital plane can form stellar shells and gaseous rings perpendicular to the major axis of the merger remnant if gaseous dissipation is included (Bekki 1997, 1998a). Thus, our future more sophisticated model with gaseous dissipation and star formation will be capable of explaining the observed HI distribution perpendicular to the photometric major axis and the outer shells as well as the above five observations. Dynamical properties of globular cluster systems and fine structures observed in NGC 5128 (Peng et al. 2002;

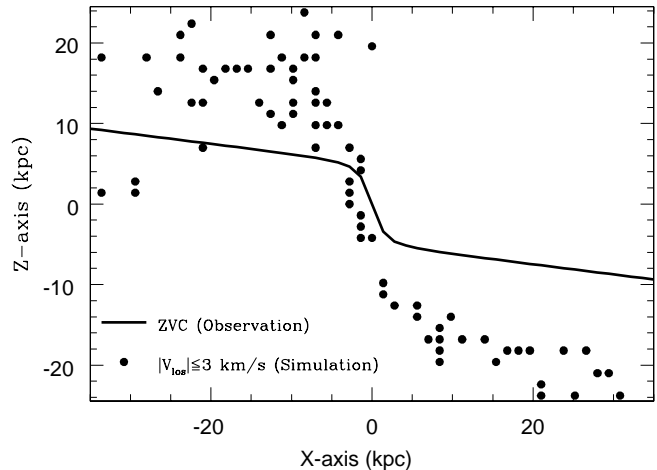


Figure 20. A comparison between the observed ZVC (zero velocity curve) and the simulated one for the model M9. The observed one (PFF04a) is represented by a solid line and the filled circles indicates the location of cells with $|V_{\text{los}}|$ (the absolute magnitude of line-of-sight-velocities) $\leq 3.0 \text{ km s}^{-1}$. The locations of the cells with $X < 0 \text{ kpc}$ and $Z < 0 \text{ kpc}$ and those with $X > 0 \text{ kpc}$ and $Z > 0 \text{ kpc}$ are not plotted for the simulation so that we can more readily infer the possible ZVC of the simulation model from the distribution of the cells with $|V_{\text{los}}| \leq 3.0 \text{ km s}^{-1}$. The mathematical expression of the observed ZVC is given in the main text.

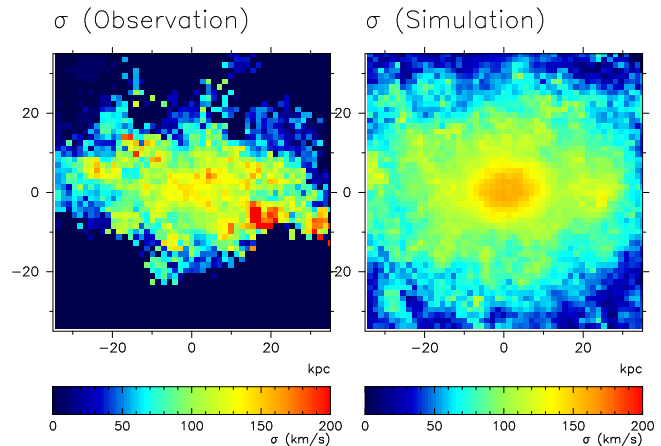


Figure 21. The same as Figure 6 but for the observational data (left) and the model M9 (right).

2004b, c) will be discussed in the best model(s) of our future studies (Bekki & Peng 2005, in preparation).

4.2 Advantages and disadvantages of the best model

Figure 19 presents the comparison between the simulated 2D velocity field of the PNS of the best model and the observed one. In order to match the observation with the simulation, the observed coordinate $-X$ (Y) for the PNS in NGC 5128 (PFF04a) is set to represent $+X$ (Z) in Figure 19 (and 20, 21) for convenience. The best model is consistent with the observation at least qualitatively in the sense that it shows (1) strong major-axis rotation extending to 35 kpc ($\approx 7R_e$), (2) weaker but significant rotation along the

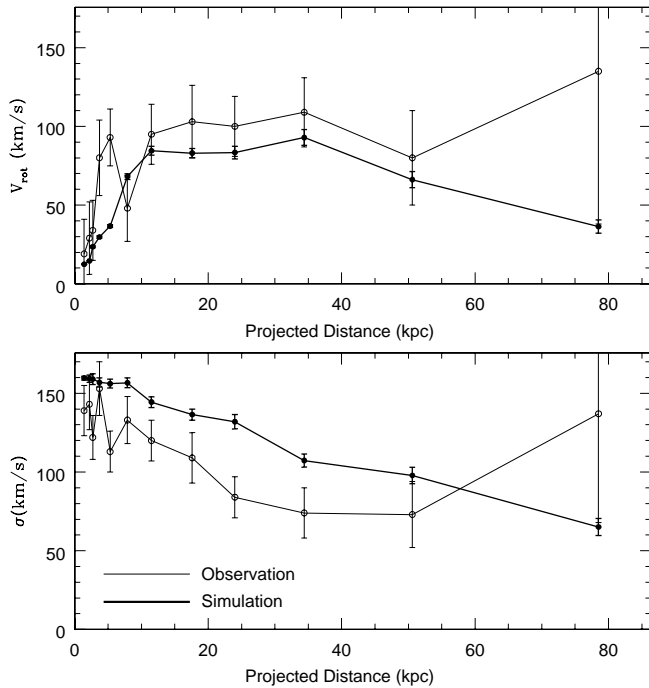


Figure 22. The same as Figure 7 but for the observational data (thin) and for the model M9 (thick). In order to compare the simulation result with the observations in a more self-consistent manner, the way of binning is exactly the same between the simulation and the observation.

minor axis, and (3) the line of zero velocity (referred to as zero velocity curve, ZVC) both misaligned and twisted with respect to the major axis of the PNe distribution.

Figure 20 more clearly describes how the ZVC looks like in the 2D velocity field and whether it is consistent quantitatively with the observed ZVC. The observed ZVC can be parameterized as follows (PFF04a):

$$Z = \frac{-X(0.125|X| + 5)}{\sqrt{(X^2 + 2.56)}} \quad (2)$$

where X and Z are exactly the same as the coordinate X and Z in the simulations. As shown in Figure 20, the simulated ZVC starts twisting at $Z \sim \pm 10$ kpc whereas the observed ZVC starts twisting at $Z \sim \pm 4$ kpc. The direction of the simulated ZVC for $|X| > 10$ kpc is broadly consistent with the observed one, though the simulated ZVC is more aligned with the minor axis of the 2D PNe distribution (shown in Figure 19) compared with the observed one for $|X| \leq 10$ kpc. These less successful reproduction of the model suggests that (1) some physics which are not included in the present study (e.g., gaseous dissipation and star formation) should be considered to reproduce fully self-consistently the observations and (2) we need to explore wider sets of model parameters (e.g., merger orbits) to find a fully self-consistent model.

Figure 21 presents the comparison between the simulated 2D velocity dispersion field of the PNS and the observed one (PFF04a). The simulation is consistent broadly with the observation in the sense that (1) it shows an inner flattened shape in the 2D velocity dispersion field and (2) radial gradient of velocity dispersion along the minor axis is steeper than that along the major axis. Interestingly, the

observation shows an isolated region with high velocity dispersion ($\sim 200 \text{ km s}^{-1}$) around $(X, Z) = (15, -5)$ (kpc). An apparently isolated region with moderately high velocity dispersion ($\sim 120 \text{ km s}^{-1}$) can be discernibly seen also in the simulation around $(X, Z) = (25, -2)$ (kpc). Although it is not so clear whether the presence of such local, dynamically hot regions in the 2D velocity dispersion fields have some physical meanings of elliptical galaxy formation, more extensive comparison between observations and simulations in terms of the locations of the isolated, dynamically hot regions should be made to determine the best model after a larger set of PNe kinematical data become available, in particular, for the regions with $X > 0$ kpc and $Z < -10$ kpc.

Figure 22 demonstrates that the best model can explain the observed rotation curve (V_{rot}) profile reasonably well for $R < 3$ kpc and $10 < R < 50$ kpc. However there is a significant difference in V_{rot} profiles between the observation and the simulation for $R \sim 5$ kpc: The observational rotation curve rises more rapidly than the simulated one for the inner region of NGC 5128. The radial profile of velocity dispersion (σ) in the model is systematically higher (a factor of 1.2 at $R \simeq 2R_e$) than the observed one. We suggest that these less successful reproduction of the best model for V_{rot} around $R = 5$ kpc and the σ profile is due to the model's not including PNe formation from gas: All PNe are assumed to originate from collisionless old stellar disks. We can expect that if PNe can form from gas, new PNe have a larger amount of rotation and smaller amount of random kinetic energy owing to efficient energy dissipation of random kinematic energy during galaxy merging. We thus suggest that our future more sophisticated model with gaseous dissipation can more successfully reproduce the observed radial profiles of V_{rot} and σ .

5 DISCUSSION

5.1 Constraints on galaxy formation from stellar halo kinematics

PFF04a have revealed that the PNS of NGC 5128 has a significant amount of rotation with V/σ between 1 to 1.5 in its outer stellar halo region ($R > 5R_e$). The present study has shown that outer stellar halos in most of major merger models have a significant amount of rotation and thus suggested that a rotating stellar halo seen in NGC 5128 is not just a special case but a rather general trend of elliptical galaxies, if ellipticals are formed by galaxy merging. The kinematics of PNSs in several elliptical galaxies have been investigated so far (Ciardullo et al. 1993; Hui et al. 1995; Arnaboldi et al. 1998; Mendez et al. 2001; Romanowsky et al. 2003; Napolitano et al. 2004; PFF04a) and found to show rotation in some of the ellipticals. Although these observational studies help the authors to provide a reasonable dynamical model (e.g., total mass of a galaxy) for each individual case, the total number of PNSs investigated is too small for them to make any robust conclusions on the general trend of kinematics in *outer stellar halos* ($R > 5R_e$) of elliptical galaxies.

We suggest that extensive systematic studies of kinematical studies of PNe for $2R_e \leq R \leq 10R_e$ for a larger number of elliptical galaxies are doubtlessly worthwhile, because the kinematics of outer stellar halos can provide strong

Table 2. Mass comparison

Model no.	Fitted mass ($M_{T,F}$)	Actual mass ($M_{T,A}$)	$M_{T,F}/M_{T,A}$
M1 (edge-on)	$1.7 \times 10^{11} M_{\odot}$	$8.6 \times 10^{11} M_{\odot}$	0.20
M1 (face-on)	$7.4 \times 10^{10} M_{\odot}$	$8.6 \times 10^{11} M_{\odot}$	0.09
M8 (edge-on)	$9.3 \times 10^{11} M_{\odot}$	$7.1 \times 10^{11} M_{\odot}$	1.31
M8 (face-on)	$1.5 \times 10^{10} M_{\odot}$	$7.1 \times 10^{11} M_{\odot}$	0.02

constraints on elliptical galaxy formation models, such as the monolithic collapse scenario (e.g., Larson 1974; Carlberg 1984) the merger one (e.g., Toomre 1977; Barnes 1992), and multiple merging of subgalactic clumps or dwarfs (e.g., Côte et al. 2002). Although kinematical properties of outer stellar halo have not been investigated by the monolithic collapse scenario (Larson 1974), it is unlikely that the outer stellar halos in elliptical galaxies formed in monolithic collapse show more rapid rotation than the inner main bodies, because random kinematical energy is likely to be dissipated away more efficiently to form a stellar system with rotation in the inner regions of protogalaxies where gas densities are higher (thus more dissipation is highly likely). If elliptical galaxies are built up through multiple merging of dwarfs with random orientation of merging, there appears to be no strong physical reasons for them to show a significant amount of rotation in their outer stellar halos. Thus stellar halo kinematics that can be proved by kinematical studies of PNSs in currently ongoing observations can be used to assess the viability of each of the above three scenarios of elliptical galaxy formation.

5.2 Halo-host connection

The present study discovered that both the radial profiles of projected PNe number densities (ρ_{PNe}) and the kinematical properties of PNSs in merger remnants depend strongly on the mass ratios of the merger progenitor spirals (See Figures 14, 15, and 16). Given the fact that morphological properties of merger remnants are demonstrated by numerical studies to depend strongly on the mass ratios (e.g., Bekki 1998b; Naab & Burkert 2003), the above discovery can provide the following three predictions on the possible correlations in dynamical properties between PNSs and their host galaxies. Firstly, more flattened E/S0 galaxies are more likely to have smaller mean ρ_{PNe} and higher V_{rot}/σ at $5R_e$, because unequal-mass galaxy mergers with $m_2 \simeq 0.3 - 0.5$ finally become more flattened E/S0s (Bekki 1998b; Naab & Burkert 2003). Secondly, stellar halos of S0s with thick disks are more likely to show a significantly smaller ρ_{PNe} compared with those of Es, because S0s with thick disks can be formed from lower mass-ratio unequal-mass galaxy mergers ($m_2 \simeq 0.1 - 0.3$). Thirdly, E/S0 galaxies can show a correlation in kinematics between V/σ (e.g., at $R \simeq 2R_e$) of the main bodies and that of their stellar halos (e.g., at $R \simeq 5R_e$), if most of them are formed from galaxy merging.

These three predictions will be more readily tested in future and ongoing kinematical studies of main bodies and stellar halos of E/S0 galaxies by the planetary nebula spectrograph (Douglas et al. 2002) and integrated field spectrographs like SAURON (Bacon et al. 2001). Furthermore, as have been demonstrated by HH00 an PFF04a, both the MDF and the kinematics of the stellar halo in NGC 5128 can be significantly different from those of the stellar halo

of the Galaxy in the sense that the stellar halo of NGC 5128 are more metal-rich and more strongly rotating. These differences in stellar halo properties may well be remarkable and fundamental differences between spiral and elliptical galaxies, though extensive observational studies of PNSs in spirals beyond the Local Group that can prove dynamical properties of the stellar halos have not been yet conducted. Although the MDF was investigated for the stellar halo of the edge-on S0 NGC 3115 (Elson 1997; Kundu & Whitmore 1998), systematic studies on the MDFs of stellar halos and dynamical properties of PNSs in S0s have not been done yet. Thus future observational studies of structural and kinematical properties of PNSs in spirals and S0s, combined with those ongoing for ellipticals, will provide a new clue to the origin of the Hubble sequence.

5.3 Mass Estimates

One ongoing field of study using PNSs is the total mass of elliptical galaxies. Typically, analysis of this sort use the integrated rotation and velocity dispersion profiles of the PNe to derive a total mass within a given radius (e.g. PFF04a, Romanowsky et al. 2003, Méndez et al. 2001). As one can see from Figure 9, a single galaxy can have a wide range of rotation and dispersion profiles depending on the viewing angle, and this could plausibly lead to biases in the mass estimation. We test this by adopting the mass estimation procedure outlined in PFF04a, which uses the spherical Jeans equation and assumes an isotropic distribution of orbits. While this is a simple assumption, it is one that is typically used and there has yet to be any strong kinematic evidence that orbits in ellipticals are strongly anisotropic. When we fit the kinematic profiles of the major merger model from the face-on and edge-on views, we find that the face-on view gives a mass that is a factor of two lower than the edge-on view. The reason for this can be seen qualitatively in Figures 7 and 8 which shows that the rotation and velocity dispersion profiles are both lower for the face-one view.

Even more intriguing, the simulations consistently show that the dark matter is at a higher velocity dispersion than the stars. In fact, while the face-on view under-represents the mass relative to the edge-on view, *both* viewing angles underestimate the total mass. In order to estimate the total mass of a merger remnant from PNe kinematics and thereby discuss this point in a more quantitatively, we use the same method as those used by Hui et al. (1995) and PFF04a: We apply the spherical Jeans equation to the major-axis rotation and line-of-sight velocity dispersion profile (e.g., Figures 7 and 8) in a merger remnant (i.e., an elliptical galaxy) to derive the dynamical mass of the remnant (See PFF04a for more details on the methods of mass estimation from PNe kinematics).

Table 2 summarizes the actual masses of the simulated E/S0s within 45 kpc ($M_{T,A}$) and the masses estimated

from the simulated radial velocity dispersion profiles and the Jeans equation used in Peng et al. (2004a) within 45 kpc ($M_{T,F}$) for two interesting cases. Compared to the total amount of mass in the simulation, our simple mass estimation from the stellar data viewed edge-on (best case) underestimates the total mass within 45 kpc by a factor of 5. In one model for a minor/unequal-mass merger viewed face-on, the total mass is underestimated by a factor of 50 and requires no dark halo. If ellipticals result from these types of mergers, then this could be a very important consideration, especially considering that current mass estimates for ellipticals are surprisingly low. This matter warrants further investigation with a variety of different elliptical formation models. (Dekel et al. 2005 have recently discussed this problem with a complementary approach and also find masses can be underestimated). However, we point out that the supposedly low M/L recently measured are for intermediate-luminosity galaxies (e.g. NGC 3379 and NGC 5128) and not for all galaxies. If this “stellar kinematic bias” is the reason for anomalously low mass estimates, then it may be more pronounced in lower luminosity ellipticals, providing a clue to their formation histories.

6 CONCLUSION

We have numerically investigated structural and kinematical properties of PNSs in elliptical galaxies formed by galaxy merging in order to elucidate the origin of the observed physical properties of PNSs. We have mainly investigated the radial profiles of projected number densities, rotational velocities, and velocity dispersion of PNSs and the two-dimensional velocity fields of PNSs in elliptical galaxies. We also compared the simulated dynamical properties of PNSs with the corresponding observations of the PNS in NGC 5128 and thereby tried to provide the best merger model for the PNS in NGC 5128. We summarize our principal results as follows.

(1) The radial densities profiles of PNSs can be fitted to the power-law in the entire halo regions of elliptical galaxies formed from major merging ($m_2 = 1.0$). The projected PNe number densities (ρ_{PNe}) at $R \sim 5R_e$ in elliptical galaxies are more than an order of magnitude higher than those of the halos of the merger progenitor spirals. These results do not depend strongly on the model parameters of major merging. The main reason for rather high ρ_{PNe} of PNSs is that a significant fraction ($\sim 10\%$) of disk stars are stripped from the disks and redistributed in the halo regions during major merging. These results suggest that elliptical galaxies have higher PNe number densities (ρ_{PNe}) in their halos than spiral ones.

(2) PNSs of elliptical galaxies formed from major merging can show a significant amount of rotation ($V_{\text{rot}}/\sigma > 0.5$) in their outer halo regions ($R > 5R_e$). The derived rotation in the outer halos results from the angular momentum redistribution of disk stars during galaxy merging (i.e., conversion of orbital angular momentum of merging two spirals into the intrinsic one of the merger remnant). V_{rot}/σ of PNSs in ellipticals are more likely to be larger in the outer parts than in the inner ones, though radial profiles of V_{rot}/σ are diverse between different models.

V_{rot}/σ at $5R_e$ can weakly correlate with V_{rot}/σ at $2R_e$ for the PNSs in such a way that PNSs with larger V_{rot}/σ at $2R_e$ are likely to show larger V_{rot}/σ at $5R_e$. This result implies that the kinematics of outer stellar halos in elliptical galaxies can correlate with that of the main bodies.

(3) The two-dimensional (2D) fields of velocity and velocity dispersion of PNSs in elliptical galaxies formed by major merging are quite diverse depending on the orbital configurations of galaxy merging, the mass ratios of the progenitor spirals, and the viewing angles of the galaxies. For example, PNSs of ellipticals formed from prograde-prograde merging can show more rapid rotation along the major axes of the PNe density profiles in their 2D velocity fields compared with the retrograde-retrograde ones. For most of the models, the 2D velocity fields show minor axis rotation in the outer halo regions of elliptical galaxies. It is doubtlessly worthwhile for future observational studies to systematically investigate dynamical properties of PNS for a larger number of elliptical galaxies and thereby to confirm whether the predicted uniformity and diversity in the 2D velocity fields of PNSs can be seen in elliptical galaxies.

(4) ρ_{PN} of PNSs are more likely to be lower in E/S0s formed from galaxy merging with smaller mass ratios (e.g., $m_2 = 0.3$, i.e., unequal-mass merging). Furthermore, PNSs in the remnants of mergers with smaller m_2 have more flattened shapes and a larger amount of rotation (V_{rot}) both in their main bodies and in their outer halos. Therefore these results suggest that more flattened E/S0s are more likely to show both lower ρ_{PNe} and higher V_{rot} (for a given luminosity range of E/S0s). This predicted correlation can be readily confirmed in future observations of PNSs.

(5) The observed kinematical properties of the PNS in NGC 5128 (e.g., V_{rot}/σ between 1 and 1.5 and minor axis rotation) can be broadly consistent with the present best model with $m_2 = 0.5$, a small impact parameter, and highly inclined initial disks (similar to a polar-orbit). The observed “kink” in the zero velocity curve (ZVC) of the 2D velocity field of the PNS in NGC 5128 can be reproduced reasonably well, though the location where ZVC begins to twist is different between the best simulation model and the observation. Some disadvantages of the present best model in explaining self-consistently the observed kinematics of the PNS suggest that gas dynamics and star formation may well play an important role in the formation of the PNS observed in NGC 5128.

(6) The mass estimates of merger remnants viewed face-on are likely to be a factor of two lower than those viewed edge-on. However, even the mass estimates of systems viewed edge-on can be low by a factor of 5, and in the worst case (face-on E/S0 model) can be low by a factor of 50. If this conclusion is applicable to real early-type galaxies, it has interesting consequences for current observational work.

ACKNOWLEDGMENTS

We are grateful to the referee for valuable comments, which contribute to improve the present paper. KB acknowledges the financial support of the Australian Research Council throughout the course of this work. The numerical simulations reported here were carried out on GRAPE systems kindly made available by the Astronomical Data Analysis Center (ADAC) at National Astronomical Observatory of Japan (NAOJ). E. W. P. acknowledges support from NSF grant AST 00-98566.

REFERENCES

- Arnaboldi, M., Freeman, K. C., Gerhard, O., Matthias, M., Kudritzki, R. P., Méndez, R. H., Capaccioli, M., & Ford, H. 1998, *ApJ*, 507, 759
- Arnaboldi, M., & Capaccioli, M. 1998, *RvMA*, 11, 129
- Bacon, R. et al. 2001, *MNRAS*, 326, 23
- Barnes, J. E. 1992, *ApJ*, 393, 484
- Barnes, J. E. 1998, in *Galaxies: Interactions and Induced Star Formation*, Saas-Fee Advanced Course 26. Springer-Verlag Berlin/Heidelberg, p275
- Beasley, M.A., Harris, W.E., Harris, G.L.H., & Forbes, D.A. 2003, *MNRAS*, 340, 341
- Bekki, K. 1997, *ApJ*, 490, L37
- Bekki, K. 1998a, *ApJ*, 499, 635
- Bekki, K. 1998b, *ApJ*, 502, L133
- Bekki, K., & Shioya, Y. 1997, *ApJ*, 478, L17
- Bekki, K., & Shioya, Y. 1998, *ApJ*, 497, 108
- Bekki, K., & Chiba, M. 2000, *ApJ*, 534, L89
- Bekki, K., & Chiba, M. 2001, *ApJ*, 558, 666
- Bekki, K., Harris, W. E., & Harris, G. L. H. 2003, *MNRAS*, 338, 587 (BHH03)
- Bendo, G. J., & Barnes, J. E. 2000, *MNRAS*, 316, 315
- Carlberg, R. G. 1984, *ApJ*, 286, 416
- Chiba, M., & Yoshii, Y. 1998, *AJ*, 115, 168
- bibitem[] Chiba, M., & Beers, T. C. 2000, *AJ*, 119, 2843
- Ciardullo, R., Jacoby, G. H., Ford, H. C., & Neill, J. D. 1989, *ApJ*, 339, 53
- Ciardullo, R., Jacoby, G. H., & Dejonghe, H. B. 1993, *ApJ*, 414, 454
- Côte, P., West, M. J., Marzke, R. O. 2002, *ApJ*, 567,853
- Couture, J, Racine, R., Harris, W. E., & Holland, S. 1995, *AJ*, 109, 2050
- Cretton, N., Naab, T., Rix, H.-W., Burkert, A., 2001, *ApJ*, 554, 291
- Davidge, T. J. 2002, *AJ*, 124, 2012
- Dekel, A., Stoehr, F., Mamon, G. A., Cox, T. J., Primack, J. R. 2005, *astro-ph/0501622*
- Douglas, N. G., et al. 2002, *PASP*, 114, 1234
- Durrell, P. R., Harris, W. E., & Pritchet, C. J. 1994, *AJ*, 108, 2114
- Durrell, P. R., Harris, W. E., & Pritchet, C. J. 2000, *AJ*, 121, 2557
- Eggen, O. J., Lynden-Bell, D., & Sandage, A. R. 1962, *ApJ*, 136, 748
- Elson, R. A. W. 1997, *MNRAS*, 286, 771
- Freeman, K. C. 1987, *ARA&A*, 25, 603
- Gregg, M. D., Ferguson, H. C., Minniti, D., Tanvir, N., & Catchpole, R. 2004, *AJ*, 127, 1441
- Grillmair, C. J., Lauer, T. R., Worthey, G., Faber, S. M., Freedman, W. L., Madore, B. F., Ajhar, E. A., Baum, W. A., Holtzman, J. A., Lynds, C. R., O'Neil, E. J. Jr., & Stetson, P. B. 1996, *AJ*, 112, 1975
- Harris, W. E., Harris, E. H., & Poole, G. B. 1999, *AJ*, 117, 855 (HHP)
- Harris, G. L. H., & Harris, W. E., 2000, *AJ*, 120, 2423 (HH00)
- Harris, W. E., & Harris, G. L. H., 2002, *AJ*, 123, 3108 (HH02)
- Heyl, J., Hernquist, L., Spergel, D. N., 1996, *ApJ*, 463, 69
- Holland, S., Fahlman, G. G., & Richer, H. B. 1996, 112, 1035
- Hui, X., Ford, H. C., Freeman, K. C., Dopita, M. A. 1995, *ApJ*, 449, 592
- Israel, F. P. 1998, *ARA&A*, 8, 237
- Larson, R. B. 1974, *MNRAS*, 166, 585
- Marleau, F. R., Graham, J. R., Liu, M. C., & Charlot, S. 2000, *AJ*, 120, 1779
- Méndez, R. H., Riffeser, A., Kudritzki, R.-P., Matthias, M., Freeman, K. C., Arnaboldi, M., Capaccioli, M., & Gerhard, O. E. 2001, *ApJ*, 563, 135
- Mould, J., & Kristian, J. 1986, *ApJ*, 305, 591
- Napolitano, N. R., Capaccioli, M., Arnaboldi, M., Merrifield, M. R., Douglas, N. G., Kuijken, K., Romanowsky, A. J., & Freeman, K. C. 2004, in *IAU Symp. 220, 'Dark Matter'*, Eds: S. D. Ryder, D. J. Pisano, M. A. Walker, and K. C. Freeman. San Francisco: Astronomical Society of the Pacific., p.173
- Naab, T., Burkert, A., 2003, *AJ*, 597, 893
- Naab, T., & Trujillo, I., 2005, accepted in *MNRAS* (*astro-ph/0508362*)
- Navarro, J. F., Frenk, C. S., & White, S. D. M., 1996, *ApJ*, 462, 563
- Norris, J. E. 1986, *ApJS*, 61, 667
- Peng, E. W., Ford, H. C., Freeman, K. C., White, R. L. 2002, *AJ*, 124, 3144
- Peng, E. W., Ford, H. C., & Freeman, K. C. 2004a, *ApJ*, 602, 685 (PFF04a)
- Peng, E. W., Ford, H. C., & Freeman, K. C. 2004b, *ApJ*, 602, 705
- Peng, E. W., Ford, H. C., & Freeman, K. C. 2004c, *ApJS*, 150, 367
- Pritchet, C. J., & van den Bergh, S. 1999, *AJ*, 118, 883
- Reitzel, D. B., Guhathakurta, P., & Gould, A. 1998, *AJ*, 116, 707
- Rejkuba, M., Minniti, D., Courbin, F., & Silva, D. R. 2002, *ApJ*, 564, 688
- Romanowsky, A. J., Douglas, N., G., Arnaboldi, M., Kuijken, K., Merrifield, M. R., Napolitano, N. R., Capaccioli, M., & Freeman, K. C. 2003, *Science*, 301, 1696
- Soria, R. et al. 1996, *ApJ*, 465, 79
- Sugimoto, D., Chikada, Y., Makino, J., Ito, T., Ebisuzaki, T., & Umemura, M. 1990, *Nat*, 345, 33
- Toomre, A., 1977, in *The evolution of galaxies and stellar Populations* ed. by B. Tinsley & R. Larson (New Haven. CN: Yale Univ. Press), p401

APPENDIX A: DERIVATION OF 2D DENSITY AND VELOCITY FIELDS

In order to compare the simulated 2D density and velocity fields with the observed ones in a more self-consistent manner, we adopt the methods that are quite similar to those used for kinematical analysis of observational data of PNSs in elliptical galaxies (e.g., PFF04a). We first determine the position angle (θ_p) of the major axis of the stellar mass distribution projected onto the x - z plane (i.e., perpendicular to orbital plane of galaxy merging) for each model at final time step. Then we rotate the model by $-\theta_p$ within the x - z plane so that the major axis of the mass distribution can coincide with the x -axis. For convenience, the coordinate (x, y, z) is renamed as (X, Y, Z) after the rotation of the model. We represent the kinematics of a model by estimating line-of-sight (LOS) velocity moments as a function of position with a nonparametric smoothing algorithm. At the position of each stellar particle, we apply a local linear smoother using a Gaussian kernel function with the smoothing length of 0.17 in our units (corresponding to 3 kpc). We choose this value of 3 kpc, firstly because recent observational study (PFF04a) chose this value and secondly because we can more clearly see the detail of the 2D velocity field of a model throughout the outer halo region (extending to $R \sim 10R_e$ without losing resolution within R_e).

We divide the entire halo region with the size of $4R_d$ ($= 70$ kpc corresponding to $\sim 14R_e$) into 50×50 cells for a merger model in each projection and estimate line-of-sight-velocity of $v(X_i, Z_i)$ for the $X - Z$ projection ($v(X_i, Y_i)$ and $v(Y_i, Z_i)$, for (X_i, Y_i) and (Y_i, Z_i) , respectively), at the center of each cell, i.e., (X_i, Z_i) ($i = 1 - 50$) based on the smoothed velocity field (described above). Total number of cells in each projection is fixed at 2500 for all merger models in the present study, because we can more clearly see the global changes of 2D velocity field without suffering small-scale, and rapid variation resulting from small number of particles in each cell for this cell number. We mainly show the 2D velocity fields projected onto the X - Y plane (referred to as the face-on view for convenience) and the X - Z plane (the edge-on plane). The same method is used for estimation the 2D density field of the PNS in model.

In converting the 2D stellar mass density field into the 2D PNe one, we assume that the luminosity-specific PNe (number) density represented as α_{PNe} is 9.4×10^{-9} PNe/ L_\odot (in B -band). This represents the number of PNe expected in the brightest 2.5 magnitudes of the PNLF, which is also roughly equivalent to the typical PN survey depth. Observations of M31's PNS (Ciardullo et al. 1989) showed that α_{PNe} can range from 2.9×10^{-9} to 39.3×10^{-9} , and accordingly the adopted value above is consistent with these observations. This value of 9.4×10^{-9} , which originates from the 2nd column of the table 4 in Ciardullo et al (1989), is used for α_{PNe} throughout this paper unless specified. While this is very obviously a simplification— α is known to vary as function of metallicity, and observational incompleteness will often vary across a galaxy—it is a good first-order approximation to the true PN population for our purposes. We also assume that $M/L_B = 3.5$ for stellar components of galaxies in all models.

The total number of PNe (N_{PNe}) within $5R_e$ of the simulated elliptical galaxies is typically ~ 350 . As shown in Fig-

ure 1, even for the small number of star particles (1000) in the halo of the disk, the initial spherical distribution of PNe (stellar halo) can be reproduced reasonably well. In most of the merger models, typically 10 % of the total stellar mass in the merger remnant can distribute throughout the halo regions ($R > 2R_e$). Therefore, more than 10^4 stellar particles (up to 5×10^4) can be used to derive the smoothed density (velocity) field for a model. Thus we can derive the smoothly changing density (velocity) fields throughout the entire halo regions from original, more discrete density (velocity) ones for the adopted total number of stellar particles in simulations by using the smoothing method described above.

We also derive the radial profiles of rotational velocity (V_{rot}) and velocity dispersion (σ) for each model based on the same method as used for observational analysis on the NGC 5128 PNS (PFF04a). For example, when we try to derive the radial profile of V_{rot} along the major axis of a PNS, we use PNe within either a perpendicular distance of ± 2 kpc from the major axis or a $\pm 10^\circ$ cone centered on the major axis. This method is adopted so that more PNe can be included in the analysis of the radial profiles for the outer halo regions, where less number of stellar particles can prevent us from making a reasonable estimate of V_{rot} and σ . The errors in V_{rot} (σ) shown in figures of the present paper (e.g., Figure 7) are equal to $V_{\text{rot}}/\sqrt{2(N-1)}$ ($\sigma/\sqrt{2(N-1)}$), where N is the total number of particles for a given radial bin. We do not intend to separately estimate V_{rot} and σ for PNe originating from spiral's stellar halos (thus metal-poor stars) and those from disks (metal-rich ones), partly because observational data sets on metallicities of PNe are not currently available. Although we find that there are no significant kinematical differences between metal-poor and metal-rich PNe in some models, we will discuss possible metallicity dependences of PNe kinematics in our forthcoming papers.

In order to investigate the smoothed 2D velocity fields, we use the same smoothing method as that used for deriving the 2D density fields of PNSs. The method of velocity smoothing is described as follows. The particle with the location \mathbf{X} , and the velocity \mathbf{V} , and the mass of M is considered to be composed of N_s particles (hereafter referred to as “smoothing particles”) that are located within R (corresponding to smoothing length) from the particle (“parent particle”) and have position vectors of \mathbf{x}_i ($i = 1 \sim N_s$) with respect to the parent, velocity vectors of \mathbf{V} (i.e., the same as that of the parent), and masses of M/N_s . The spatial distribution of these smoothing particles with respect to the parent particle (\mathbf{X}) follows the Gaussian distributions. Therefore the probability of a i -th smoothing particle with the position of $\mathbf{X} + \mathbf{x}_i$ is proportional to $\exp(-r_i^2/2R^2)$, where r_i is the distance between the parent particle and the smoothing one. If the number of smoothing particles for a stellar particle is 100, the total number of “particles” used for 2500 bins is about 10^6 . Therefore, each bin includes 400 “particles” on average.

For each bin, we average the velocities of “particles” with the positions within the bin and derive the velocity at the location of the bin. The adopted smoothing length is consistent with that used for observations by PFF04a. Also we confirm that this method can reproduce the “spider shape” (which is characteristic of rotational kinematics) of the 2D velocity field of the initial disk. Thanks to this smoothing method, we can derive 2D density, velocity, and dispersion

fields of PNSs that can be tested against the corresponding observations in a fully self-consistent manner.

This study is based totally on dissipationless simulations of galaxy mergers so that it can not discuss structure and kinematics of PNe formed from gas during/after galaxy merging. Accordingly, the present results can be more reasonably compared with the observed E/SOs formed from “dry” (dissipationless) mergers that do not create new PNe. In our future papers, we will discuss how the introduction of PNe formation in our numerical simulations can change main conclusions derived in the present study.

APPENDIX B: MULTIPLE MERGERS

Each multiple merger model contains equal-mass spiral galaxies with random orientations of intrinsic spin vectors which are uniformly distributed within a sphere of size $6R_d$. The most important parameter in this multiple merger model is the ratio of the initial kinematic energy (T_{kin}) of the merger to that of initial potential (W). By varying this ratio (t_v ; defined as $|2T_{\text{kin}}/W|$) from 0.25 to 0.75, we investigate how t_v controls the final PNe kinematics of the merger remnants. We mainly investigate the results of two extreme cases: (1) where the initial kinetic energy of a multiple merger is due entirely to the random motion of the five constituent galaxies (referred to as “dispersion supported”) and (2) where it is due entirely to (rigid) rotational motion (“rotation supported”). Our investigation of these two cases enables us to understand how the initial rotation (dispersion) can control the final kinematical properties of PNe in merger remnants.

Although we have derived the results of three models with $t_v = 0.25, 0.5$, and 0.75 for each case (i.e., six models in total), we describe the result of the “rotation supported” model with $t_v = 0.5$ (labeled as M10 in the Table 1). This is firstly because this multiple merger model show some interesting differences in PNe kinematics compared with pair merger models, and secondary because this model shows typical behaviors in PNe kinematics among multiple merger models. The merger remnant of this rotation supported model shows a flattened stellar (thus PNe) distribution if it is seen from edge-on and have effective radius of 11.4 kpc for the stars and 29.8 kpc for the dark matter halo.

We briefly summarize the results as follows. The radial gradient in σ is significantly shallower in the multiple merger models than in pair merger models. These shallower σ profiles in PNe kinematics can be seen in most multiple models and thus can be regarded as one of characteristics of PNSs in multiple merger remnants. The difference in σ at each radial bin between PNe and dark matter halo is slightly larger than that seen in pair merger models. Both dark matter halo and PNe show larger rotational velocities in the outer part of the halo and PNe can show larger V_{rot} than dark matter halo.

Thus PNSs in elliptical galaxies formed by multiple mergers show similar kinematics to those in elliptical galaxies by pair mergers, though the maximum values of σ and V_{rot} can be different between the two cases owing to the larger masses in multiple mergers. Remarkable differences in PNe kinematics between the two different merger mod-

els are (1) shallower slopes of radial σ profiles in multiple merger models and (2) larger σ differences between dark matter halo and PNe for the multiple merger model. The above (1) suggests that there can be diversity in radial σ profiles in elliptical galaxies, *if most of elliptical galaxies are formed either from pair mergers or from multiple ones*. The above (2) implies that radial σ profiles of PNSs alone can not allow us to correctly estimate of the total masses of elliptical galaxies formed by multiple merging. We have a plan to investigate this problem related to mass estimation of galaxies by PNe kinematics in a more extensive manner in our forthcoming papers (Bekki & Peng 2005)